

Recent flavour-physics results in open charm decays

Wei Xu^{a,*} for BESIII Collaboration

*^aInstitute of High Energy Physics, Chinese Academy of Sciences
19B Yuquan Road, Shijingshan District, Beijing, China*

E-mail: xuwei@ihep.ac.cn

The BESIII experiment has accumulated 2.93 fb^{-1} of data at the $\psi(3770)$ peak for the study of $D^{0\pm}$ decays, 7.33 fb^{-1} of data at \sqrt{s} in the range of $[4.128, 4.226] \text{ GeV}$ for the study of $D_s^{(*)\pm}$ decays, and 4.5 fb^{-1} of data at \sqrt{s} in the range of $[4.6, 4.7] \text{ GeV}$ for the study of Λ_c^\pm decays. Based on these data samples, we report the measurements for the leptonic, semi-leptonic, and hadronic decay of charmed hadrons.

*The 21st International Conference on B-Physics at Frontier Machines - BEAUTY2023
3-7 July 2023
Clermont-Ferrand, Lyon, France*

*Speaker

1. Introduction

The leptonic decay of charmed meson can be factorized in terms of strong and weak interactions. Therefore, the determination of the leptonic decay rate measures production of the CKM element $|V_{cq}|$ and the decay constant $f_{D_q^+}$ directly [1], which allows us to test CKM unitarity or Lattice quantum chromodynamics (LQCD) calculations. Incorporating decay widths of $D_q^+ \rightarrow \mu\nu_\mu$ [2] and $D_q^+ \rightarrow \tau\nu_\tau$ [2] allow lepton flavor universality (LFU) to be tested [1]. Currently, the measurements are consistent with SM predictions considering the uncertainties.

Similarly, the semi-leptonic decay can also be separated into a strong and weak part. Incorporating the input from LQCD [1], we can also test the CKM unitarity by measuring the decay width. Alternatively, the LQCD calculations can be tested in various q^2 region by inputting $|V_{cq}|$ from the CKMfitter Group. The LFU can also be tested with the differential decay width. In addition, the forward-backward asymmetry parameters can provide a critical test of LFU with small sensitivity to uncertainties from the form factor parametrizations [3]. Hadronic decay of charmed hadrons can not only deliver information on the charmed hadrons itself but also the final states. Measurements of the branching fractions provide inputs for the study of bottom hadron decays and calibrations for the non-perturbative QCD models. Incorporating different decay channels, the SU(3) breaking effect can be studied. By studying the final state with amplitude analyses, one can study the light hadron spectroscopy and interaction of the light hadrons.

The BESIII experiment provides clean environment for the study of charmed hadrons. Its detector [4] records symmetric e^+e^- collisions provided by the BEPCII storage ring [5]. The single-tag (ST) [6] and the double-tag (DT) technique [6] are used in the reconstruction of the charmed hadrons.

2. Leptonic decays

2.1 $D_s^+ \rightarrow \tau^+\nu_\tau$

Recently, $D_s^+ \rightarrow \tau^+\nu_\tau$ via $\tau^+ \rightarrow \mu^+\nu_\mu\bar{\nu}_\tau$ and $\tau^+ \rightarrow \pi^+\bar{\nu}_\tau$ decays have been studied via the process $e^+e^- \rightarrow D_s^{*\pm}D_s^\mp$ [7, 8]. The branching fractions are measured with the two τ decay modes. In particular, the results of the measurement with $\pi^-\bar{\nu}_\tau$ supersede the previous BESIII results [9]. To discriminate the signal for $\pi^+\bar{\nu}_\tau$ modes from the background, a boost decision tree is applied. The values of $f_{D_s^+}|V_{cs}|$ are determined with measured branching fraction $\mathcal{B}(D_s^+ \rightarrow \tau^+\nu_\tau)$. The values of $f_{D_s^+}$ and $|V_{cs}|$ are also determined separately. The BESIII results are the most precise measurements available of $f_{D_s^+}$ and $|V_{cs}|$. The LFU is also tested, but there is no significant violation being observed.

2.2 $D_s^{*+} \rightarrow e^+\nu_e$

The $D_s^{*+} \rightarrow e^+\nu_e$ decay is observed with a statistical significance of 2.9σ [10]. It is the first hint of leptonic decay of excited charmed strange meson. The branching fraction $\mathcal{B}(D_s^{*+} \rightarrow e^+\nu_e)$ is measured to be $(2.1_{-0.9}^{+1.2} \pm 0.2_{\text{syst}}) \times 10^{-5}$, corresponding to an upper limit of 4.0×10^{-5} at the 90% confidence level. The total width of the D_s^{*+} meson is determined to be $(121.9_{-52.2}^{+69.6} \pm 11.8)$ eV, which agrees with the prediction from LQCD. The upper limit for the decay width is constrained from

MeV [2] to the keV level. The decay constant is determined to be $(213.6^{+61.0}_{-45.8\text{stat.}} \pm 43.9_{\text{syst.}})$ MeV, which offers the first experimental test on various theory models.

3. Semi-leptonic decays

3.1 $D_s^+ \rightarrow f_0(980)e^+\nu_e$

The branching fraction of this decay is measured to be $(1.72 \pm 0.13_{\text{stat.}} \pm 0.10_{\text{syst.}}) \times 10^{-3}$ with an improved precision [11]. Assuming $f_0(980)$ to be a regular $q\bar{q}$ state, the measured branching fraction implies the $s\bar{s}$ component is dominant in the $q\bar{q}$ mixing picture of $f_0(980)$. In addition, the differential branching fraction is measured in different q^2 regions. The form factor $f_+^{f_0}(q^2)$ is modeled by the simple pole parametrization. By fitting the differential decay width, the $f_+^{f_0}(0)|V_{cs}|$ is determined to be $0.504 \pm 0.017_{\text{stat.}} \pm 0.035_{\text{syst.}}$ for the first time. Using $|V_{cs}| = 0.97349 \pm 0.00016$ [2], the form factor $f_+^{f_0}(0) = 0.518 \pm 0.018_{\text{stat.}} \pm 0.036_{\text{syst.}}$ is obtained and can be compared to various theoretical predictions. The measurement is consistent with predictions from CLFD [12], DR [12] and QCDSR [13, 14]. However, it is much larger than the calculations from LCSR [15], LFQM [16], and CCQM [17].

3.2 $\Lambda_c^+ \rightarrow \Lambda l^+\nu_l (l = e, \mu)$

The decays $\Lambda_c^+ \rightarrow \Lambda l^+\nu_l (l = e \text{ and } \mu)$ are studied simultaneously [3, 18]. Improved measurements of $\mathcal{B}(\Lambda_c^+ \rightarrow \Lambda l^+\nu_l)$ are performed. Comparing to the predictions, the theory models in the Refs [19, 20] are disfavored at a confidence level of more than 95%.

The q^2 dependent LFU tests are performed with the measured differential width and forward-backward asymmetry parameters. There is no significant violation of LFU since the results are consistent with the LQCD predictions. Using the forward-backward asymmetry parameter, the Λ_c decay asymmetry parameter is determined model-independently for the first time. The results are consistent with the LQCD prediction. The measured q^2 dependent form factors show different kinematic behavior and provide an important test and calibration for the LQCD. A test for T asymmetry is also performed and no indication of new physics is observed.

4. Hadronic decays

4.1 Inclusive decay of $D_q^{0/+}$

Measured branching fractions of the inclusive decays of $D_q^{0/+}$ are mesons summarized in Table 1 [21–23]. Comparisons with the corresponding sum of branching fractions of the observed exclusive decay modes indicate that there are still unobserved decay modes. For the $D_s^+ \rightarrow \pi^+\pi^+\pi^-X$ decay, the differential branching fraction as a function of the $M_{\pi^+\pi^+\pi^-}$ is also measured.

4.2 $D^+ \rightarrow K_S^0\pi^+\pi^0\pi^0$

The first amplitude analysis of $D^+ \rightarrow K_S^0\pi^+\pi^0\pi^0$ is performed [24]. The dominant intermediate processes are determined to be $D^+ \rightarrow K_S^0 a_1(1260)^+(\rightarrow \rho^+\pi^0)$ and $D^+ \rightarrow \bar{K}^{*0}\rho^+$ with branching fractions of $(8.66 \pm 1.04_{\text{stat.}} \pm 1.39_{\text{syst.}}) \times 10^{-3}$ and $(9.70 \pm 0.81_{\text{stat.}} \pm 0.53_{\text{syst.}}) \times 10^{-3}$, respectively. The total branching fraction is measured to be $(2.888 \pm 0.058_{\text{stat.}} \pm 0.069_{\text{syst.}})\%$.

Table 1: Comparisons between measured inclusive branching fraction \mathcal{B}_{inc} , sum of observed exclusive branching fractions $\mathcal{B}_{\text{exc}}^{\text{sum}}$ [2], and corresponding difference $\Delta\mathcal{B}$.

Decay Mode	\mathcal{B}_{inc} (%)	$\mathcal{B}_{\text{exc}}^{\text{sum}}$ (%)	$\Delta\mathcal{B}$ (%)
$D^0 \rightarrow K_S^0 X$	$32.78 \pm 0.13 \pm 0.27$	31.68 ± 0.32	1.10 ± 0.41
$D^+ \rightarrow K_S^0 X$	$20.54 \pm 0.12 \pm 0.18$	18.16 ± 0.72	2.38 ± 0.75
$D^0 \rightarrow \pi^+ \pi^+ \pi^- X$	$17.60 \pm 0.11 \pm 0.22$	16.05 ± 0.47	1.55 ± 0.53
$D^+ \rightarrow \pi^+ \pi^+ \pi^- X$	$15.25 \pm 0.09 \pm 0.18$	14.74 ± 0.53	0.51 ± 0.53
$D_s^+ \rightarrow \pi^+ \pi^+ \pi^- X$	$32.81 \pm 0.35 \pm 0.82$	24.7 ± 1.5	8.11 ± 1.74

4.3 $D_s^+ \rightarrow K_S^0 K_S^0 \pi^+$

An amplitude analysis of the $D_s^+ \rightarrow K_S^0 K_S^0 \pi^+$ decay is performed [25] for the first time. A structure around $1.7 \text{ GeV}/c^2$ in the $M_{K_S^0 K_S^0}$ distribution is observed as shown in Fig. 1a. The obtained mass and width are consistent with corresponding values of $f_0(1710)$ [2]. However, the branching fraction of $D_s^+ \rightarrow S(1710)\pi^+$ is one order of magnitude larger than the expectation based on isospin symmetry and $\mathcal{B}(D_s^+ \rightarrow f_0(1710)\pi^+, f_0(1710) \rightarrow K^+ K^-)$ [26]. This large enhancement can likely be attributed to constructive interference between $a_0(1710)$ and $f_0(1710)$, which interfere destructively in the charged decay mode $D_s^+ \rightarrow f_0(1710)\pi^+$. There is no significant contribution of $D_s^+ \rightarrow S(980)\pi^+, S(980) \rightarrow K_S^0 K_S^0$ in the $D_s^+ \rightarrow K_S^0 K_S^0 \pi^+$, while $S(980)$ is observed in $D_s^+ \rightarrow K^+ K^- \pi^+$ with a significance greater than 20σ . The larger difference can also be explained by the interference between $a_0(980)$ and $f_0(980)$. A simultaneous amplitude analysis of the two decay modes can further clarify this situation.

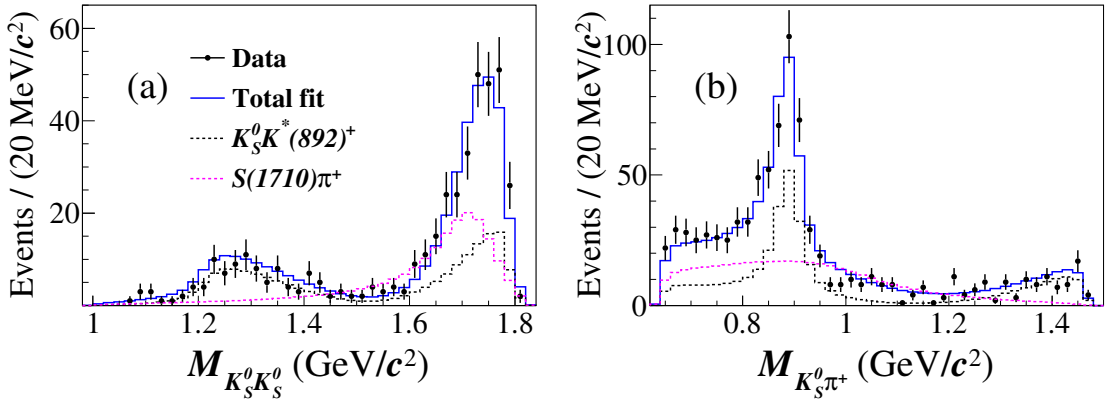


Figure 1: Distribution of (a) $M_{K_S^0 K_S^0}$ and (b) $M_{K_S^0 \pi^+}$ from the nominal fit. The distribution of $M_{K_S^0 \pi^+}$ contains two entries per event, one for each K_S^0 . The data samples are represented by points with uncertainties and the fit results by the blue lines. Colored dashed lines show the individual components of the fit model. Due to interference effects, the total PDF is not necessarily equal to the sum of the components [25].

4.4 $D_s^+ \rightarrow K_S^0 K^+ \pi^0$

An amplitude analysis of the $D_s^+ \rightarrow K_S^0 K^+ \pi^0$ decay is performed [27]. A a_0 -like structure is observed in the $M_{K_S^0 K^+}$ distribution, as shown in Fig. 2a. The mass and width are measured to be

$(1.817 \pm 0.008_{\text{stat.}} \pm 0.020_{\text{syst.}}) \text{ GeV}/c^2$ and $(0.097 \pm 0.022_{\text{stat.}} \pm 0.015_{\text{syst.}}) \text{ GeV}$. The branching fraction $\mathcal{B}(D_s^+ \rightarrow a_0(1817)^+\pi^0)$ is determined to be $(3.44 \pm 0.52 \pm 0.32) \times 10^{-3}$. Along with the branching fraction of $\mathcal{B}(D_s^+ \rightarrow S(1710)\pi^+)$, the structure can be interpreted as an isospin-1 partner of $f_0(1710)$ [27]. However, there is about a $100 \text{ MeV}/c^2$ difference from the predicted value, which implies instead that the observed a_0 -like structure is the isospin-one partner of $X(1812)$ observed in the $J/\psi \rightarrow \gamma\omega\phi$ decay [27]. Finally, a precise measurement of branching fraction of $\mathcal{B}(D_s^+ \rightarrow K_S^0 K^+\pi^0) = (1.46 \pm 0.06_{\text{stat.}} \pm 0.05_{\text{syst.}})\%$ is obtained with an improvement in the precision compared to previous analysis by a factor of 2.8.

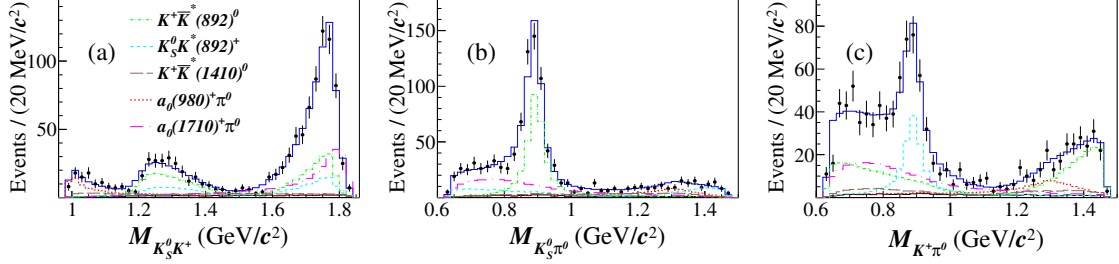


Figure 2: The projections of the Dalitz plot onto (a) $M_{K_S^0 K^+}$, (b) $M_{K_S^0 \pi^0}$, and (c) $M_{K^+ \pi^0}$. The data samples are represented by points with error bars, the fit results by blue lines, and backgrounds by black lines. Colored dashed lines show the components of the fit model. Because of interference effects, the fit results are not necessarily equal to the sum of the components [27].

4.5 $\Lambda_c^+ \rightarrow \Lambda\pi^+\pi^0$

A partial wave analysis of the $\Lambda_c^+ \rightarrow \Lambda\pi^+\pi^0$ decay is performed [28]. The dominant contributions of intermediate processes are from $\Lambda_c^+ \rightarrow \Lambda\rho(770)^+$, $\Lambda_c^+ \rightarrow \Sigma(1385)^+\pi^0$, and $\Lambda_c^+ \rightarrow \Sigma(1385)^0\pi^+$ decays, which are observed for the first time. Making use of $\mathcal{B}(\Lambda_c^+ \rightarrow \Lambda\pi^+\pi^0)$ from the Particle Data Group [2], the branching fractions and decay asymmetry parameters are measured. The results are compared with various theoretical predictions but no theoretical model provides results which are consistent with both the measured branching fraction and decay asymmetry parameters.

5. Summary

Recently, the BESIII experiment has made a lot of progress in the study of charmed hadron decays. For the leptonic and semi-leptonic decays, branching fraction and differential decay width are measured. Based on these results, various theoretical predictions are tested. Two structures, $S(1710)$ and $S(1817)$, are observed in the amplitude analyses. In the future, more clean data will be collected for the study of charmed hadrons. Specifically, data at $\psi(3770)$ resonance corresponding an integrated luminosity of 20 fb^{-1} will be available in 2024. In the near future, it is expected that more results with higher precision will be reported.

References

- [1] H. B. Li and X. R. Lyu, *Natl. Sci. Rev.* **8**, nwab181 (2021).

- [2] R. L. Workman *et al.* (Particle Data Group), *PTEP* **2022**, 083C01 (2022).
- [3] M. Ablikim *et al.* (BESIII Collaboration), *Phys. Rev. D* **108**, L031105 (2023).
- [4] M. Ablikim *et al.* (BESIII Collaboration), *Nucl. Instrum. Meth. A* **614**, 345 (2010).
- [5] C. H. Yu *et al.* (JACoW, Geneva, Switzerland, 2016) doi:10.18429/JACoW-IPAC2016-TUYA01.
- [6] J. Adler *et al.* (MARK-III Collaboration), *Phys. Rev. Lett.* **60**, 89 (1988).
- [7] M. Ablikim *et al.* (BESIII Collaboration), *Phys. Rev. D* **108**, 092014 (2023).
- [8] M. Ablikim *et al.* (BESIII Collaboration), *J. High Energy Physics* **09**, 124 (2023).
- [9] M. Ablikim *et al.* (BESIII Collaboration), *Phys. Rev. D* **104**, 052009 (2021).
- [10] M. Ablikim *et al.* (BESIII Collaboration), *Phys. Rev. Lett.* **131**, 141802 (2023).
- [11] M. Ablikim *et al.* (BESIII Collaboration), *Phys. Rev. Lett.* **132**, 141901 (2024).
- [12] B. El-Bennich *et al.*, *Phys. Rev. D* **79**, 076004 (2009).
- [13] I. Bediaga, F. S. Navarra, and M. Nielsen, *Phys. Lett. B* **579**, 59 (2004).
- [14] T. M. Aliev and M. Savci, *EPL* **90**, 61001 (2010).
- [15] P. Colangelo, F. De Fazio, and W. Wang, *Phys. Rev. D* **81**, 074001 (2010).
- [16] H. W. Ke, X. Q. Li, and Z. T. Wei, *Phys. Rev. D* **80**, 074030 (2009).
- [17] N. Soni *et al.*, *Phys. Rev. D* **102**, 016013 (2020).
- [18] M. Ablikim *et al.* (BESIII Collaboration), *Phys. Rev. Lett.* **129**, 231803 (2022).
- [19] T. Gutsche *et al.*, *Phys. Rev. D* **93**, 034008 (2016).
- [20] M. Pervin, W. Roberts, and S. Capstick, *Phys. Rev. C* **72**, 035201 (2005).
- [21] M. Ablikim *et al.* (BESIII Collaboration), *Phys. Rev. D* **107**, 032002 (2023).
- [22] M. Ablikim *et al.* (BESIII Collaboration), *Phys. Rev. D* **108**, 032001 (2023).
- [23] M. Ablikim *et al.* (BESIII Collaboration), *Phys. Rev. D* **107**, 112005 (2023).
- [24] M. Ablikim *et al.* (BESIII Collaboration), *J. High Energy Physics* **09**, 077 (2023).
- [25] M. Ablikim *et al.* (BESIII Collaboration), *Phys. Rev. D* **105**, L051103 (2022).
- [26] M. Ablikim *et al.* (BESIII Collaboration), *Phys. Rev. D* **104**, 012016 (2021).
- [27] M. Ablikim *et al.* (BESIII Collaboration), *Phys. Rev. Lett.* **129**, 182001 (2022).
- [28] M. Ablikim *et al.* (BESIII Collaboration), *J. High Energy Physics* **12**, 033 (2022).